ELSEVIER

Journal of Organometallic Chemistry 571 (1998) 231–241

Journal of Organometallic Chemistry

Rhodium COD complexes of mixed donor set tripod ligands: coordination chemistry and catalysis[1]

Albrecht Jacobi, Gottfried Huttner *, Ute Winterhalter

Anorganisch-Chemisches Institut der Universität Heidelberg, Im Neuenheimer Feld 270, D-69120 Heidelberg, Germany

Received 19 May 1998

Abstract

The reaction of the novel mixed tripod ligands $RCH_2C(CH_2X)(CH_2Y)(CH_2Z)$ **1**–**6** (X, Y, Z = PPh_2, NR_2, pyrazol-1-yl; R = H, OH) with $[Rh^I(COD)Cl]_2$ is investigated. The resulting rhodium COD complexes $[(\mathbf{1}–\mathbf{6})Rh(COD)]PF_6$, **7** are characterized by NMR spectroscopy, mass spectra and elemental analysis. In addition, X-ray structure analysis is performed on several compounds **7**, where in contrast to the behavior of the parent compound triphos $[MeC(CH_2PPh_2)_3]$, the potential tripod ligands **2**–**6** are found to coordinate in a bidentate mode. $\{\eta^2$-*P*,*O*-$[HOCH_2C(CH_2PPh_2)(CH_2NEt_2)_2]Rh(COD)]\}PF_6$, **7i** exhibits the first structurally characterized example of an intramolecular hydrogen bond between a non-coordinated and a coordinated donor atom. The activities of the complexes **7** as catalyst precursors in the homogeneous hydrogenation of diphenylacetylene and (*Z*)-α-*N*-acetamidocinnamic acid are tested and rationalized with respect to a proposed reaction mechanism. © 1998 Elsevier Science S.A. All rights reserved.

Keywords: Mixed donor set ligands; Rhodium COD complexes; Hydrogen bonding; Hydrogenation

1. Introduction

Neopentane based tripod ligands of the general constitution $RC(CH_2X)(CH_2Y)(CH_2Z)$ with X, Y, Z being donor groups have been shown to complex transition metals in a facial coordination mode [1]. In their metal templates, tripod-M, one half of the coordination sphere is blocked effectively by the ligand cage, while the individual types of donor groups affect the shape of the remaining coordination space [2]. This fact, together with the prominent ability of trisphosphanes (e.g. triphos) to stabilize various transition metals in different oxidation states [1], makes tripod ligands ideal candidates for catalytic applications [3]. However, it was found for rhodium catalized hydrogenation and hydroformylation reactions of olefins, that the trihapto coordination mode, which is preferred by neopentane based trisphosphane ligands, is more of an impediment for this type of catalytic transformation ([3]c, [4]).

This result can mainly be ascribed to the in general nondissociative character of η^3-chelating triphos, which leaves the corresponding fragments unable to create free coordination sites at the metal center ([3]c). In the case of an 'arm-off' process, as recently found under hydroformylation conditions [5], where one of the three phosphine arms in triphos creates a free site for substrate binding, the similarity of the phosphine donors with respect to their kinetic lability makes the formation of the active η^2-coordinated species an unselective process ([4]d).

In the case of bidentate chelate ligands, a way to faciliate and possibly even control this dissociation process, is the use of hemilabile ligands with two electronically different donor groups (e.g. phosphine and phosphinoxide, amine or ether functions) ([6]). In addition, this type of ligands with soft and hard donor

* Corresponding author. Tel.: +49 622 1548481; fax: +49 622 1545707.

[1] Dedicated to Prof. Dr. Dr. h.c. muet. E.O. Fischer on the occasion of his 80th birthday.

PII S0022-328X(98)00882-1

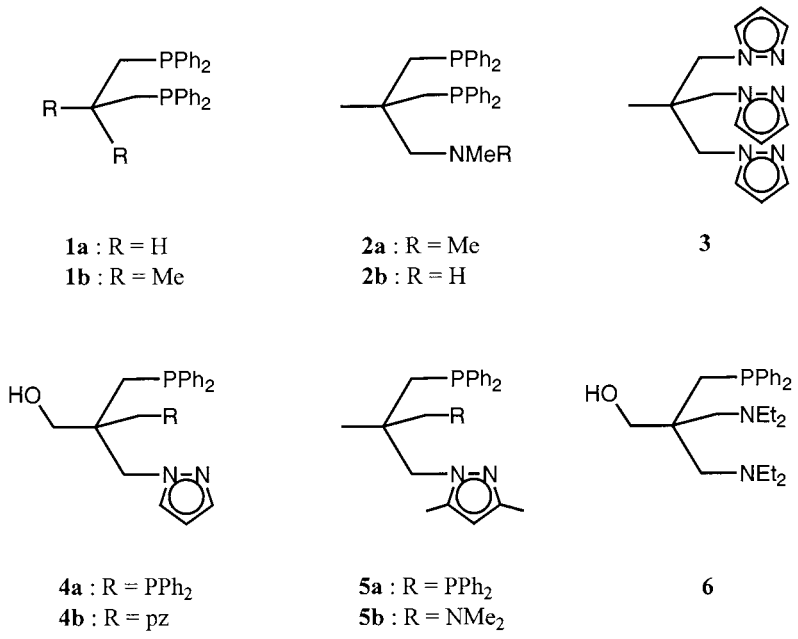

Scheme 1.

functions creates distinctive electronic conditions at the reactive positions *trans* to a certain donor function at the metal. This can lead to higher selectivities, as shown for example in the industrial synthesis of α-olefins (SHOP ([6]b)) (Scheme 1).

Herein we report the synthesis and structural characterisation of rhodium(I) complexes with mixed-donor set hemilabile ligands which are potential tripods [7]. In addition, rhodium(I) complexes of the chelating diphos ligands **1a** (dppp) and **1b** are prepared as standard catalyst precursors to be compared with the hemilabile systems.

2. Results and discussion

The synthesis of rhodium(I) complexes **7** was performed according to a modified literature procedure ([4]d). The diphos ligands of type **1** react with half an equivalent of di-μ-chloro-bis-(η^4-1,5-cyclooctadiene)-dirhodium(I) ([8]) and one equivalent of potassium hexafluorophosphate to form the complexes **7a** and **7b** (Scheme 2). The presence of a pseudo-four-coordinate structure in **7a** and **7b,** where the metal center is surrounded by a chelating diphos and the COD coligand, can be deduced from their respective NMR data:

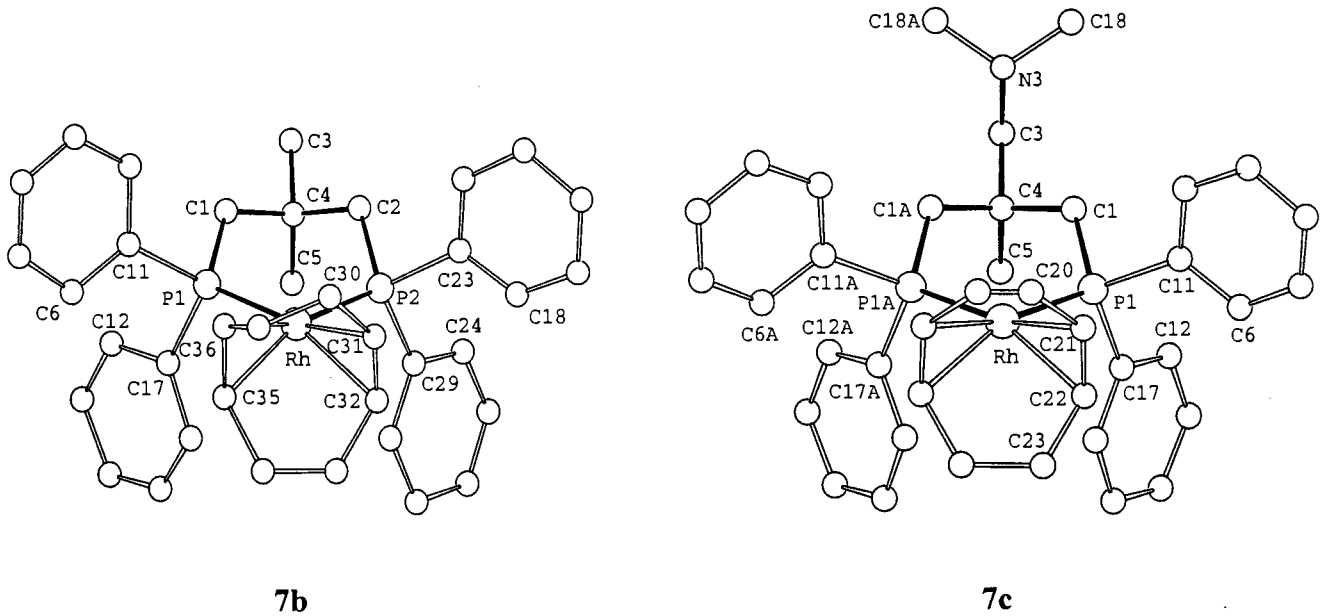

7b **7c**

Fig. 1. Molecular structure of the cations of **7b** and **7c** in the solid state. Selected bond distances (pm), bond angles (°) and torsion angles (°).

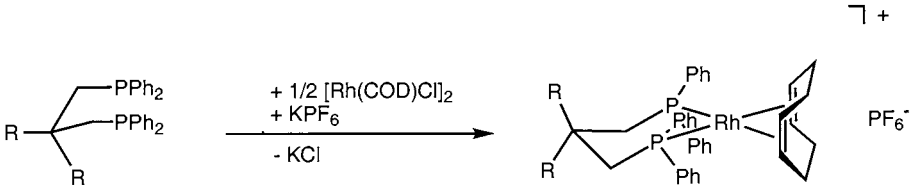

7a : R = R' = H
7b : R = R' = Me
7c : R = CH_2NMe_2, R' = CH_3
7d : R = CH_2NMeH, R' = CH_3
7e : R = CH_2(3,5Me_2pz), R' = CH_2OH

Scheme 2.

The ^{31}P-NMR spectra of **7a** and **7b** show just one doublet at small positive δ values which is in accord with two chemically equivalent phosphorus atoms coupled to ^{103}Rh and a septet for the PF_6^- counterion at δ around −145 (see Section 3) [9]. Consistently two broad signals with a 2:1 ratio for the methylene and the olefinic COD protons are found in their ^{1}H-NMR spectra (see Section 3). Crystals of **7b** which were suitable for X-ray diffraction could be obtained after column chromatography of the crude product over silica gel with dichloromethane/diethylether 1:1 and vapour gas diffusion of petroleum ether 40/60 into a dichloromethane solution of purified **7b**.

The mixed donor set PPN tripod ligands **2a**, **2b** and **4a** show a coordination behavior at the rhodium center which is similar to the one observed for the diphos ligands **1**. The respective ^{31}P-NMR spectra of the new complexes **7c**, **7d** and **7e** again show just one doublet at positive δ values (c. f. **7a**, **7b**). The fact, that the amine donor is not coordinated in these compounds and thus is in a dangling arm position is prooved by X-ray structure determination in the case of **7c** (see below).

While **7b** is found to crystalize in spacegroup $P2_1$ with one molecule in the crystallographically independent unit, in **7c** the mirror plane of its crystallographic space group $P2_1/m$ is found as a symmetry element of the cation (Fig. 1, Table 1). Despite this fact, the conformations of **7b** and **7c** in the solid state are very similar (Fig. 1, Table 1). In both cases the ligands react to form six membered chelate rings in a chair conformation with the phenyl rings in an achiral arrangement (see Table 1, torsion angles). The coordination of the metal center is pseudo square planar and the Rh–P bond lengths and P–Rh–P angles are in the expected range in each case (Table 1) [9]. The relative positions of the coligand in **7b** and **7c** as well as the orientation of the phenyl rings at the phosphorus centers are comparable. In conclusion, the dangling amino arm function in **7c** does not seem to influence the coordination sphere of the metal in these complexes. The conformation of the COD ligands in **7b** and **7c** is different (Fig. 1). Conformations of both types have previously been reported in the literature ([4]c).

Complex **7d** is obtained as a yellow microcrystalline solid, while **7e** is a viscous, orange-coloured oil; any attempt to grow single crystals suitable for X-ray diffraction failed. However, a comparison of the NMR data of **7c** with the data of **7d** and **7e** leads to the proposal of an analoguos η^2-*P*,*P* coordination mode for the PPN ligands in **7d** and **7e** (Scheme 2).

Ligand **3** reacts with half an equivalent of di-μ-chloro-bis-(η^4-1,5-cyclooctadiene)-dirhodium(I) and one equivalent of potassium hexafluorophosphate to form the compound **7f** (Scheme 3). After chromatographic workup and recrystallisation **7f** can be obtained in high yield in the form of large yellow crystals suitable for X-ray structure analysis. It is found, that the potentially tripodal ligand **3** is forming a pseudo square planar coordination sphere at the rhodium, leaving one pyrazolyl donor uncoordinated (Fig. 2).

While this type of η^2-coordination was observed for Pt(II) [10] and Pd(II) [11] complexes of tris-(pyrazol-1-yl)methane (with a fast exchange of coordinated and

Table 1
Selected bond distances (pm), bond angles (°) and torsion angles (°) for **7b**, and **7c**

7b		**7c**	
Rh–P1	230.3(4)	Rh–P1	230.3(2)
Rh–P2	231.7(4)		
Rh–C31	221.1(17)	Rh–C21	224.6(8)
Rh–C32	229.8(17)	Rh–C22	224.0(8)
Rh–C35	218.7(18)		
Rh–C36	232.0(17)		
P1–Rh–P2	90.7(1)	P1–Rh–P1A	89.4(1)
P1–Rh–C31/C32	93.5	P1–Rh–C21/C22	93.1
P2–Rh–C35/C36	92.0		
Rh–P1–C11–C6	−96.1(13)	Rh–P1A–C11A–C6A	−100.1(7)
Rh–P1–C17–C12	0.0(12)	Rh–P1A–C17A–C12A	−173.8(6)
Rh–P2–C23–C18	90.1(14)	Rh–P1–C11–C6	100.1(7)
Rh–P2–C29–C24	−179.3(14)	Rh–P1–C17–C12	173.8(6)

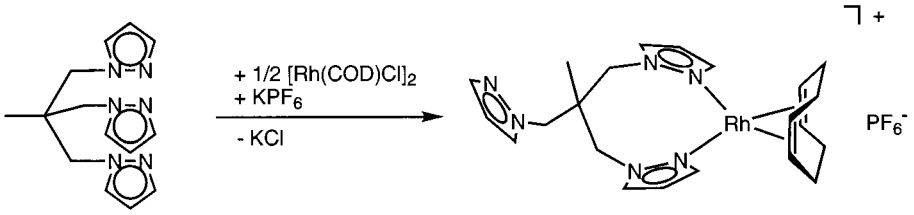

3 7f

Scheme 3.

uncoordinated donors in the case of Pd(II)), [Ir(COD)Cl]$_2$ reacts with tris-(pyrazol-1-yl)methane to form η^2- as well as η^3-coordinated derivatives, which equilibrate in solution [12]. In contrast to the complexes of tris-(pyrazol-1-yl)methane, which form six membered chelate rings, ligand **3** necessarily forms an eight membered chelate cycle in **7f** (Fig. 2). The conformation of the ring is comparable to an extended chair form. As a consequence of the hybridisation of the aromatic pyrazol systems, the ring atoms C1, N11, N1 and Rh as well as C2, N22, N2 and Rh, respectively lie in one plane (Fig. 2). The bite angle of the ligand is with 84.9° significantly smaller than the bite angle in the six membered diphos chelates of **7b** and **7c** (see above). The weak *trans* effect of the nitrogen donors in **7f** gives rise to much shorter Rh–C(COD) bonds than in **7b** and **7c**, where the olefins are in competition with phosphorus donor groups (Fig. 2, Table 1).

In order to obtain hemilabile rhodium complexes with both, hard and soft donor functions coordinating to the metal center, PNN ligands **4b**, **5b** and **6** were used in complexation reactions of the above type. Ligand **5b** is of the standard neopentane tripod type, while **4b** and **6** have an additional OH function at the backbone, that is as well capable of interacting with the metal center ([6]a). Ligands **4b**, **5b** and **6** react with the rhodium salt to form complexes **7g**, **7h** and **7i** as yellow–orange coloured microcrystalline solids (Schemes 4 and 5). The metal coordination of the phosphorus donor can in all three cases be deduced

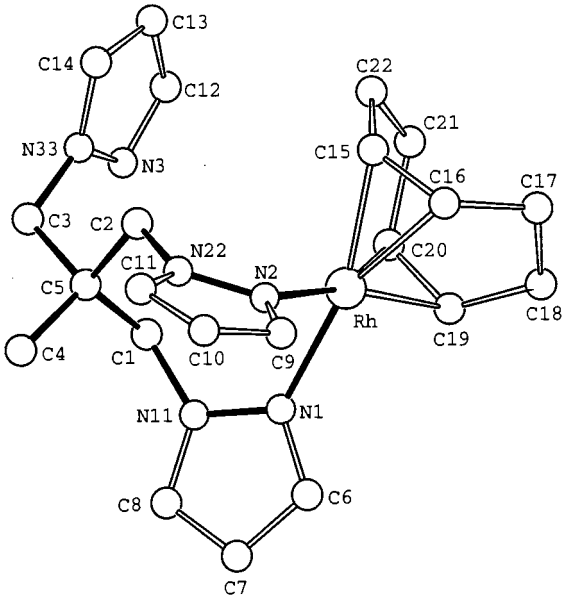

7f

Fig. 2. Molecular structure of **7f** in the solid state. Selected bond distances (pm), bond angles (°) and torsion angles (°): Rh–N1 211.2(2), Rh–N2 208.7(2), Rh–C15 211.5(3), Rh–C16 214.1(2), Rh–C19 213.1(2), Rh–C20 213.7(2), C15–C16 138.6(4), C19–C20 138.9(4), N1–Rh–N2 84.9(1), N1–Rh–C19/C20 95.2, N2–Rh–C15/C16 92.5, N1–N11–N22–N2–5.8, Rh–N1–N11–C1 23.6(3), Rh–N2–N22–C2 −7.8(3).

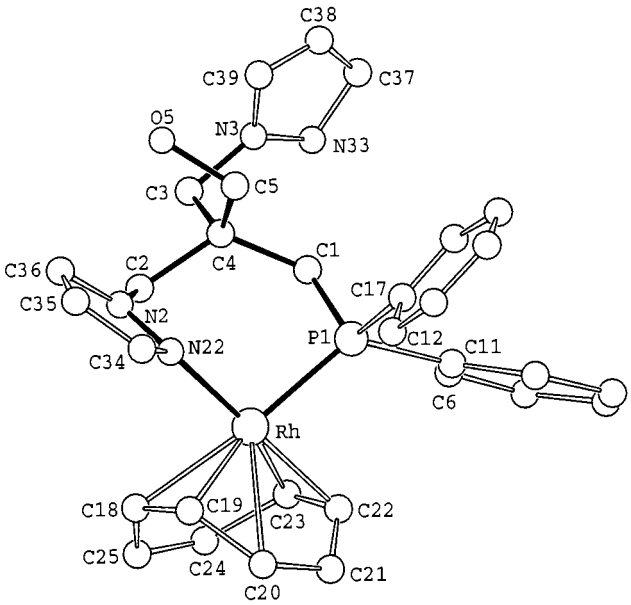

7g

Fig. 3. Molecular structure of **7g** in the solid state. Selected bond distances (pm), bond angles (°) and torsion angles (°): Rh–P1 229.4 (5),Rh–N22 212.9(13), Rh–C18 240.4(20), Rh–C19 201.4(14), Rh–C22 214.6(13), Rh–C23 211.7(14), P1–Rh–N22 99.8(3), P1–Rh–C18/C19 85.7, N22–Rh–C22/C23 80.4, Rh–N22–N2–C2 −20.2(17), N22–N2–C2–C4 −67.2(14), N2–C2–C4–C1 102.4(14), C2–C4–C1–P1 −62.6(16), C4–C1–P1–Rh 45.5(12), C1–P1–Rh–N22 −60.9(12), P1–Rh–N22–N2 68.7(14), Rh–P1–C11–C6 72.5(11), Rh–P1–C17–C12 15.9(16).

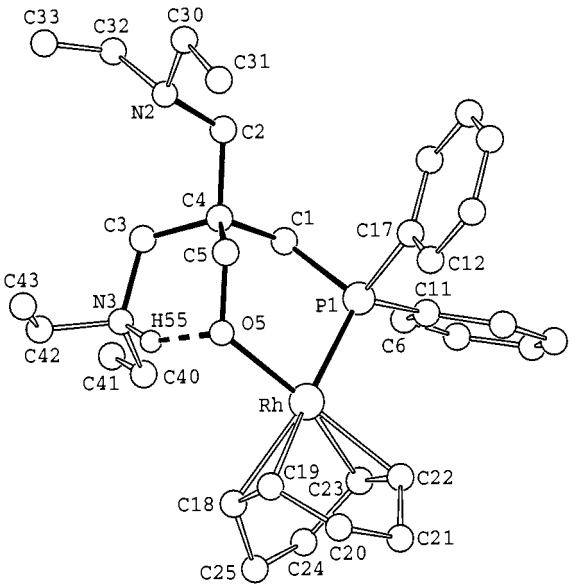

7i

Fig. 4. Molecular structure of **7i** in the solid state. Selected bond distances (pm), bond angles (°) and torsion angles (°): Rh–P1 227.0(1), Rh–O1 204.3(2), Rh–C18 225.3(3), Rh–C19 223.0(3), Rh–C22 213.2(3), Rh–C23 211.4(3), N3–H55 106.7, O5–H55 160.4, N3–H55–O5 148.7, P1–Rh–O5 89.0(1), P1–Rh–C18/C19 96.4, O5–Rh–C22/C23 87.8, Rh–P1–C1–C4 53.1(2), P1–C1–C4–C5 −4.1(4), C1–C4–C5–O5 −63.7(4), C4–C5–O5–Rh 72.9(3), C5–O5–Rh–P1 −14.0(2), O5–Rh–P1–C1 −39.6(1), P1–C1–C5–O5 −59.1, O5–C5–C3–N3 13.6, Rh–P1–C11–C6 88.4(3), Rh–P1–C17–C12 16.3(3).

from an upfield shift in the ^{31}P-NMR spectra of $\Delta\delta$ around 45 ppm compared to the free ligand [9]. In addition a ^{1}J(Rh,P) coupling of around 150 Hz is found in each case (see Section 3). The interpretation of the ^{1}H-NMR spectra (200 MHz) of **7g**, **7h** and **7i** poses some difficulties as the low energy barrier for the rotation of the COD coligand leads to broad signals for the olefinic and methylene protons which strongly overlap with the methylene groups of the tripod ligand ([4]c). Nevertheless, the signal groups in the ^{1}H-NMR spectra of **7g**, **7h** and **7i** show the expected integral ratios (see Section 3).

Single crystals of **7g** are obtained after recrystallisation from dichloromethane at 0°C (see Section 3). Due to bad crystal quality and disordered solvent molecules, the result of the crystal structure analysis of **7g** allows only for a qualitative interpretation of the structural features (see Table 4). The hydroxy tripod ligand **4b** is found in an η^2-*P*,*N*-coordination mode (Fig. 3). A comparison of the chelate cycle in **7g** with the crystal structure of **4b***Mo(CO)$_4$ ([7]b), in which the ligand is found to be η^2-*P*,*N*-coordinated as well, shows an increase of the bite angle from around 88° in **4b***Mo(CO)$_4$ to around 100° in **7g**.

In the case of the *PNN′* tripod ligand **5b** the question, whether the aromatic or the aliphatic amine function is coordinated in addition to the phosphorus donor in complex **7h**, cannot be answered unambiguously. The ^{1}H-NMR spectrum does not allow to differentiate between coordinated and uncoordinated donor groups due to strong overlapping in the aliphatic region (see Section 3).

The coordination behavior of the *PNN* hydroxy tripod ligand **6** incorporating one PPh_2 group and two NEt_2 groups is in strong contrast to the results found with **4b** at Rh(I) (Figs. 3 and 4). The X-ray structure of complex **7i** exhibits an η^2-*P*,*O* binding mode, the metal again being in a pseudo square planar geometry (Fig. 4). The P1–Rh–O5 bite angle of 89° is in the range found for chelating bisphosphanes in the compounds **7b** and **7c** while the Rh–P1 bond length is with 227 pm somewhat shorter than usual (Fig. 4). The weak *trans* effect of the oxygen donor is reflected by a significant shortening of the Rh–C bonds *trans* to O1 (212 pm) compared to the Rh–C bonds *trans* to P1 (224 pm). The alcohol function of the ligand is deprotonated upon coordination, while one of the amino groups is protonated and thus acting as a proton donor in a hydrogen bond with the metal bound oxygen (Fig. 4). The second NEt_2 group in **7i** is not coordinated and points away from the metal center. The bridging hydrogen H55 was located by difference Fourier techniques and its position was refined by least-squares. Although this hydrogen bond is strong in the solid state (d_{N-O} = 257 pm), no signal could be assigned in the ^{1}H-NMR spectrum (probably due to strong overlap in the aliphatic region) nor could an appropriate band be found in the IR spectrum of **7i**. The hydrogen bond seems to influence the six-membered chelate cycle, which is found in an unusual twisted boat form, as indicated by the respective torsion angles (Fig. 4) [13]. The adjacent six-membered cycle built up by hydrogen bonding is in a clear boat type arrangement, which is described by a small torsion angle O5–C5–C3–N3 of only 13.6° (Fig. 4).

The torsion angles Rh–P1–C11–C6 and Rh–P1–C17–C12 account for the rotational position of the two phenyl groups at P1. They are closely similar for the complexes **7g** and **7i**, although these two compounds incorporate different chelate ring sizes and bite angles (Figs. 3 and 4).

This finding is probably caused by the steric interaction of one phenyl ring with the bulky COD coligand, which restricts the value of Rh–P1–C11–C6 to around 80°. A small value of Rh–P1–C17–C12 (around 16°) is found as a consequence of the gearing of the phenyl rings at P1 (Fig. 4) ([2]a).

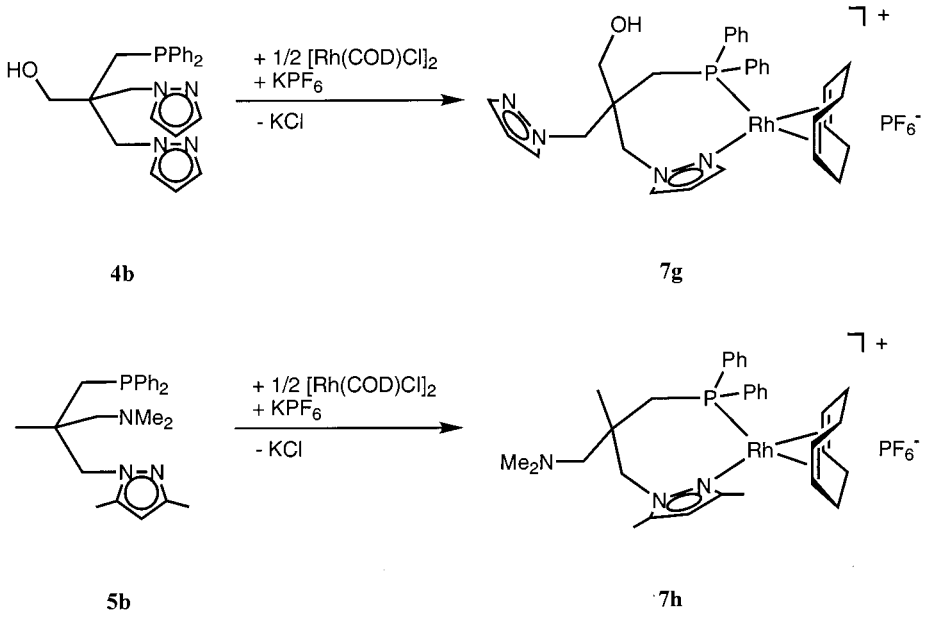

Scheme 4.

3. Catalysis

Tripod rhodium complexes with three electronically equivalent donors were employed in catalytic hydrogenations of various olefins ([3]a–d, [4]c, d, [14]). While chelating olefins of the enamide type showed poor results with all systems tested ([4]c, d, [14]), the hydrogenation of simple non-chelating olefins such as 1-hexene proved more active with [(triphos)RhH(C_2H_4)] ([3]c). This is presumably due to the fact, that non-chelating olefines need no phosphine dissociation to accomplish the hydrogenation reaction.

On the other hand, the Halpern-mechanism for the catalytic hydrogenation of chelating enamides with diphos rhodium complexes [15] would, in adaption to a tripodal system, require the dissociation of one coordinative bond (not admitting the intermediacy of 20-electron species) to allow the addition of H_2 [16]. In the proposed substrate catalyst complex ([4]d) this dissociation could affect either one of the tripod donor groups or the olefin carbonyl function.

In order to test this hypothesis, the hemilabile Rh(I) systems **7** were used in the hydrogenation of diphenylacetylene and (*Z*)-α-*N*-acetamidocinnamic acid. The conversion rates for the hydrogenation of diphenylacetylene with compounds **7** are found to be lower than the rates obtained for triphos rhodium compounds (Table 2) ([3]c). The diphos system **7a** is the most active, while the presence of additional N or O donor groups seems to inhibit the reaction (Table 2). Complex **7g**, forming a *P*,*N* chelate, is almost as active as the *P*,*P* chelate **7c**, which means, that a diphos fragment is not neccessary to obtain catalytic activity. **7g** is also the only catalyst producing an appreciable amount of *cis*-stilbene, although the product distributions cannot be rationalized with the data at hand ([3]c).

The hydrogenation of (*Z*)-α-*N*-acetamidocinnamic acid was performed in an hydrogenation apparatus, which allowed the measurement of the H_2 consumption. In contrast to the results for the hydrogenation of diphenylacetylene, the compounds incorporating a pyrazolyl residue were all catalytically inactive (no conversion after 120 h, see Table 3). While **7b** with the neopentane diphos chelate affected quantitative conversion of the substrate in only 20 min, the hemilabile PPN system **7c** took 1.5 h and the tripodal [(triphos)Rh-

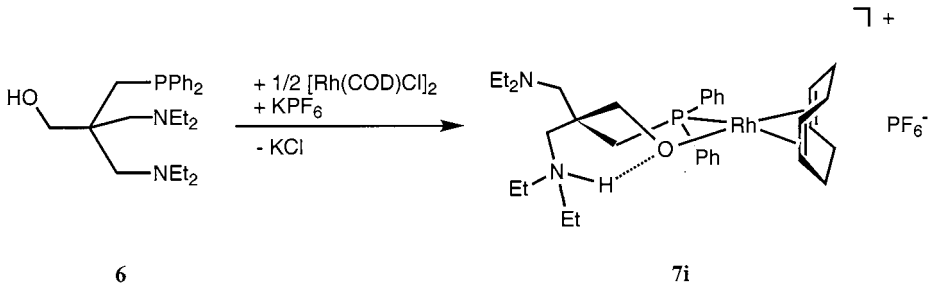

Scheme 5.

Table 2
Hydrogenation of diphenylacetylene

Catalyst	Conversion (%)	Crude composition[a]			
		1,2-Diphenylethane (%)	*cis*-Stilbene (%)	*trans*-Stilbene (%)	Diphenylacetylene (%)
7a	83	46	<5	33	17
7c[b]	50	8	<5	40	51
7e[c]	22	9	<5	9	78
7g[d]	42	10	14	18	58

Reaction conditions, 2 mmol diphenylacetylene; 0.02 mmol catalyst; 25 ml THF; 20°C; hydrogen pressure 30 bar; reaction time 3 h; 1 mol% catalyst.
[a] The fraction of *cis*-stilbene was only roughly estimated due to overlapping signals in the aromatic region (200 MHz).
[b] 1 Bar, 100% conversion after 4 days.
[c] 1 Bar, 100% conversion after 5 days.
[d] 1 Bar, 100% conversion after 5 days.

(COD)]PF_6 reached 100% conversion only after 168 h (Table 3). This order of reactivity supports the proposed dissociation of either a solvent molecule (**7b**) or a donor group of the ligand {**7b**, [(triphos)Rh-(COD)]PF_6} as the rate determining step during the catalytic cycle [15,16]. In accordance with this idea, breaking a labile Rh–N bond in catalyst **7b** is more facile than breaking a Rh–P bond in [(triphos)-Rh(COD)]PF_6 and leads to a strongly increased activity of **7b**.

Finally, it must be stated that the rhodium catalysed hydrogenation does not seem to be the right choice of a catalytic application for the new hemilabile tripod ligands. Nevertheless it was shown, that a lot of different coordination modes can be realised with the various *P*,*N* ligands, including a new type of 'secondary' interaction of a free donor group with a metal bound donor group in the case of **7i** [17]. Thus the concept of hemilabile chelate ligands can be extended to tripod ligands, making the finding of new applications for this concept a worthwhile task.

4. Experimental part

4.1. General

All manipulations were carried out under an argon atmosphere by means of standard Schlenk techniques. Solvents were dried by standard methods [18] and distilled under argon. The solvents $CDCl_3$ and CD_2Cl_2 used for the NMR spectroscopic measurements were degassed by three successive 'freeze-pump-thaw' cycles and dried over 4-Å molecular sieves. NMR: Bruker Avance DPX 200 at 200.13 MHz (^{1}H), 50.323 MHz (^{13}C{^{1}H}), 81.015 MHz (^{31}P{^{1}H}), T = 298K, chemical shifts (δ) in ppm with respect to $CHCl_3$ (^{1}H: $\delta = 7.27$, ^{13}C: $\delta = 77.0$) and CH_2Cl_2 (^{1}H: $\delta = 5.32$, ^{13}C: $\delta = 53.5$) as internal standards. ^{31}P chemical shifts (δ) in ppm with respect to 85% H_3PO_4 (^{31}P: $\delta = 0$) as external standard. MS (EI): Finnigan MAT 8320; Fast-Atom-Bombardment (FAB) xenon, matrix: 4-nitrobenzyl-alcohol. Melting points (m.p.): Gallenkamp MFB-595 010, melting points are uncorrected. Elemental analyses: Microanalytical Laboratory of the Organisch-Chemisches Institut, Universität Heidelberg. The silica gel (Kieselgel z.A. 0.06–0.2 mm, J.T. Baker Chemicals B.V.) used for chromatography was degassed at 1 mbar for 24 h and saturated with argon. Di-μ-chloro-bis-(η^4-1,5-cyclooctadiene)-dirhodium(I) was prepared according to a literature procedure [8]. 1,3-Bis-(diphenylphosphanyl)propane and 2,2-bis-(diphenylphosphanylmethyl)propane were purchased from Lancaster Chemicals. All other chemicals were obtained from commercial suppliers and used without further purification.

4.2. X-ray structure determinations

The measurements were carried out on a Siemens P4 four circle diffractometer (equipped with a low temperature device) with graphite monochromated Mo–K_α radiation. All calculations were performed using the SHELXT PLUS [19] software package. Structures were solved by direct methods with the SHELXS-86 program ([19]a) and refined with the SHELX-93 program ([19]b). Graphical handling of the structural data dur-

Table 3
Hydrogenation of (*Z*)-α-*N*-acetamidocinnamic acid

Catalyst	Reaction time (h)	Conversion (%)
[(Triphos)Rh(COD)]PF_6	168	100
7a	20	100
7b	0.3	100
7c	1.5	100
7e	120	0
7f	120	0
7g	120	0

Reaction conditions, 1 mmol AAC; 25 ml MeOH; 20°C; 1 bar H_2; 1 mol% catalyst.

Table 4
Crystal data for **7b**, **7c**, **7f**, **7g**, and **7i**

Compound	**7b**	**7c**	**7f**	**7g**	**7i**
Formula	$C_{37}H_{42}P_3F_6Rh$	$C_{39}H_{47}NP_3F_6Rh$	$C_{22}H_{30}N_6F_6Rh$	$C_{31}H_{37}N_4OP_2F_6Rh*CH_2Cl_2^*Et_2O$	$C_{33}H_{51}N_2P_2F_6Rh$
Molecular mass (g)	796.53	839.63	626.39	760.50	770.62
Crystal size (mm)	$0.2\times0.2\times0.25$	$0.3\times0.3\times0.2$	$0.3\times0.3\times0.1$	$0.2\times0.1\times0.2$	$0.4\times0.4\times0.3$
Crystal system	Monoclinic	Monoclinic	Triclinic	Monoclinic	Monoclinic
Space group (no.)	$P2_1$ (4)	$P2_1/m$ (11)	$P\bar{1}$ (2)	$P2_1$ (4)	$P2_1/c$ (14)
a (pm)	112.38(1)	108.67(3)	94.12(3)	94.61(2)	128.44(1)
b (pm)	150.85(1)	174.30(5)	108.41(4)	174.91(3)	98.26(2)
c (pm)	114.21(2)	116.97(3)	130.75(4)	221.38(6)	281.31(4)
α (°)	90	90	74.13(2)	90	90
β (°)	112.55(1)	107.72(1)	76.98(1)	81.03(2)	100.65(1)
γ (°)	90	90	83.05(2)	90	90
V (10^6 pm^3)	1788.1(4)	2110.4(10)	1247.8(7)	3618.6(14)	3489.1(9)
Z	2	2	2	2	4
$D_{calc.}$ (g cm^{-3})	1.479	1.447	1.667	1.527	1.448
T (K)	298	200	200	200	200
No. of reflections for cell parameter refinment	37	25	25	25	48
Scan range	$3.9\leq2\theta\leq52.0°$	$4.3\leq2\theta\leq50.0°$	$3.9\leq2\theta\leq50.5°$	$4.4\leq2\theta\leq56.5°$	$5.1\leq2\theta\leq51.0°$
Scan speed (° min^{-1})	$\omega=7$	$\omega=8$	$\omega=5$	$\omega=12$	$\omega=8$
No. of reflections measured	3840	4051	4786	6048	6785
No. of unique reflections	3654	3839	4486	5676	6485
No. of reflections observed	2903	2863	4062	2829	5362
Observation criterion	$I=2\sigma$	$I=2\sigma$	$I=2\sigma$	$I=2\sigma$	$I=2\sigma$
No. of parameters refined	438	337	445	441	427
Residual electron density (10^{-6}e pm^{-3})	0.68	1.10	0.77	1.88	0.73
R_1/R_w (%) (refinement on F^2)	3.5/9.4	6.9/18.5	2.5/6.2	12.8/26.6[a]	3.7/10.7

[a] Due to badly resolved, disordered solvent molecules.

ing solution and refinement was done with XPMA [20]. An absorption correction (ψ-scan, $\Delta\psi=10°$) was applied to all data. Atomic coordinates and anisotropic parameters of the non-hydrogen atoms were refined by full-matrix least-squares calculations. Data for the structure determination are compiled in Table 4.

4.3. [1,3-Bis-(diphenylphosphanyl)propane-rhodium(I)-η^4-1,5-cyclooctadiene]hexafluoro-phosphate (7a)

A total of 247 mg (0.5 mmol) di-μ-chloro-bis-(η^4-1,5-cyclooctadiene)-dirhodium(I) was dissolved in 5 ml dichloromethane. In a second flask 190 mg (1.03 mmol) potassium hexafluorophosphate was dissolved in 5 ml acetone adding 0.2 ml of water. This solution was added to the orange-coloured rhodium(I) solution. A colourless potassium chloride precipitate was formed during 5 min, while the colour of the reaction mixture faded. A total of 412 mg (1 mmol) 1,3-bis-(diphenylphosphanyl)propane **1a** ([8]a) in 5 ml dichloromethane was then added. After stirring at room temperature for 1 h, the solvents were removed in vacuo (10^{-1} mbar). The residue was taken up in acetone and dried over sodium sulfate. The insoluble potassium chloride was removed by filtering the solution over kieselgur. The resulting orange-coloured solution was chromatographed over silica gel. After elution of small amounts of side products (not further characterized) with dichloromethane, the main product was eluted with dichloromethane/diethylether 1:1 as a sharp orange-coloured band, which gave upon removal of the solvent 570 mg (0.74 mmol, 74%) **7a** as an orange-coloured microcrystalline solid, m.p. 190°C (decomposition). Anal. Found: C, 53.86; H, 5.42; P, 11.94. $C_{35}H_{38}P_3F_6Rh$ (768.50): Anal. Calc.: C, 54.70; H, 4.98; P, 12.09%. ^{1}H-NMR (CD_2Cl_2): 2.01–2.79 [m, 12H, methylene-*H*(COD), C*H*$_2$P], 4.65 [bs, 4H, olefin-*H*(COD)], 7.20–7.58 (m, 20H, aromatic H). ^{13}C-NMR: no spectrum obtained because of the low solubility of **7a** in CD_2Cl_2. ^{31}P-NMR (CD_2Cl_2): +8.2 (d, 2P, $^1J_{RhP}=142$ Hz), −145.6 (sept, 1P, $^1J_{PF}=712$ Hz, PF_6^-).

4.4. [2,2-Bis-(diphenylphosphanylmethyl)-propane-rhodium(I)-η^4-1,5-cyclooctadiene]hexafluorophosphate (7b)

Compound **7b** was prepared as described above for **7a**. Starting materials: 440 mg (1 mmol), 2,2-bis-(diphenylphosphanylmethyl)-propane **1b** ([8]b), 247 mg (0.5 mmol) di-μ-chloro-bis-(η^4-1,5-cyclooctadiene)-dirhodium(I), 190 mg (1.03 mmol) potassium hexa-

fluorophosphate. Chromatographic workup (see above) gave upon removal of the solvent 570 mg (0.71 mmol, 71%) **7b** as an orange-coloured microcrystalline solid. Recrystallisation afforded 500 mg (0.63 mmol, 63%) of **7b** in the form of orange-coloured crystals suitable for X-ray structural analysis, m.p. 179°C (decomposition). Anal. Found: C, 55.61; H, 5.59; P, 11.54. $C_{37}H_{42}P_3F_6Rh$ (796.56): Anal. Calc.: C, 55.79; H, 5.31; P, 11.67%. ^{1}H-NMR (CD_2Cl_2): 0.69 (s, 6H, CqCH_3), 2.37–2.47 [m, 12H, methylene-*H*(COD), CH_2P], 4.58 [bs, 4H, olefin–*H*(COD)], 7.22–7.74 (m, 20H, aromatic H). ^{13}C-NMR: no spectrum obtained because of the low solubility of **7b** in CD_2Cl_2. ^{31}P-NMR (CD_2Cl_2): + 15.1(d, 2P, $^1J_{RhP} = 142$ Hz), − 144.1 (sept, 1P, $^1J_{PF} = 712$ Hz, PF_6^-).

4.5. η^2-P,P-[2,2-Bis-(diphenylphosphanylmethyl)-dimethylpropanamin-rhodium(I)-η^4-1,5-cyclooctadiene]-hexafluorophosphate (7c)

Compound **7c** was prepared as described above for **7a**. Starting materials: 484 mg (1 mmol) **2a** ([7]a), 247 mg (0.5 mmol) di-μ-chloro-bis-(η^4-1,5-cyclooctadiene)-dirhodium(I), 190 mg (1.03 mmol) potassium hexafluorophosphate. Chromatographic workup (see above) gave upon removal of the solvent 490 mg (0.58 mmol, 58%) **7c** as an orange-coloured microcrystalline solid. Recrystallisation afforded 400 mg (0.48 mmol, 48%) of **7c** in the form of orange-coloured crystals suitable for X-ray structural analysis, m.p. 165°C. Anal. Found: C, 55.69; H, 5.78; N, 1.60; P, 10.97. $C_{39}H_{47}NP_3F_6Rh$ (839.63): Anal. Calc.: C, 55.79; H, 5.64; N, 1.67; P, 11.07%. MS (FAB), *m*/*z* (%) [frag.]: 694 (100) [{(**2a**)Rh(COD)}$^+$], 586 (92) [{(**2a**)Rh}$^+$], 509 (22) [{(**2a**)Rh}$^+$–Ph], 401 (23) [{(**2a**)Rh}$^+$–PPh_2]. ^{1}H-NMR ($CDCl_3$): 0.39 (s, 3H, CqCH_3), 1.73–2.70 (m, 20H, methylene–*H*(COD), CH_2P, CH_2N, NMe_2), 4.28, 5.39 [2bs, 4H, olefin–*H*(COD)], 7.07–7.89 (m, 20H, aromatic *H*). ^{13}C-NMR ($CDCl_3$): 27.1 (bs, Cq*C*H_3), 30,5 [bs, $C_{methylene}$(*COD*)], 34.4 (m, *C*H_2P), 40.9 (s, *C*q), 49.1 (s, N*C*H_3), 75.2 (m, *C*H_2N), 100.0, 104.4 [2bs, C_{olefin}(*COD*)], 128.5–135.1 (m, aromatic *C*). ^{31}P-NMR ($CDCl_3$): + 13.8 (d, 2P, $^1J_{RhP} = 141$ Hz), − 144.2 (sept, 1P, $^1J_{PF} = 712$ Hz, PF_6^-).

4.6. η^2-P,P-[2,2-Bis-(diphenylphosphanylmethyl)-methylpropanamin-rhodium(I)-η^4-1,5-cyclooctadiene]-hexafluorophosphate (7d)

Compound **7d** was prepared as described above for **7a**. Starting materials: 470 mg (1 mmol) **2b** ([7]a), 247 mg (0.5 mmol) di-μ-chloro-bis-(η^4-1,5-cyclooctadiene)-dirhodium(I), 190 mg (1.03 mmol) potassium hexafluorophosphate. Chromatographic workup (see above) allowed the elution of **7d** as a sharp yellow band with dichloromethane/THF 1:1 which gave upon removal of the solvent 590 mg (0.71 mmol, 71%) **7d** as a yellow microcrystalline solid. m.p. 185°C (decomposition). Anal. Found[2]: C, 51.26; H, 5.24; N, 1.54. $C_{38}H_{45}NP_3F_6Rh$ (825.60): Anal. Calc.: C, 55.28; H, 5.49; N, 1.70%. MS (FAB), *m*/*z* (%) [frag.]: 680 (100) [{(**2b**)Rh(COD)}$^+$], 572 (29) [{(**2b**)Rh}$^+$], 494 (37) [{(**2b**)Rh}$^+$–Ph]. ^{1}H-NMR ($CDCl_3$): 0.50 (s, 3H, CqCH_3), 1.15 (bs, N*H*), 1.99–2.60 (m, 17H, methylene-*H*(COD), CH_2P, CH_2N, N*Me*), 4.52 [bs, 4H, Olefin-*H(COD)*], 7.30–7.78 (m, 20H, aromatic *H*). ^{13}C-NMR: no spectrum obtained because of the low solubility of **7d**. ^{31}P-NMR ($CDCl_3$): + 13.7 (d, 2P, $^1J_{RhP} = 141$ Hz), − 144.2 (sept, 1P, $^1J_{PF} = 712$ Hz, PF_6^-).

4.7. η^2-(P,P)-[2,2-Bis-(diphenylphosphanylmethyl)-2-(pyrazol-1-yl-methyl)-1-propanol-rhodium(I)-η^4-1,5-cyclooctadiene]hexafluorophosphate (7e)

Compound **7e** was prepared as described above for **7a**. Starting materials: 525 mg (1 mmol) **4a** ([7]b), 247 mg (0.5 mmol) di-μ-chloro-bis-(η^4-1,5-cyclooctadiene)-dirhodium(I), 190 mg (1.03 mmol) potassium hexafluorophosphate. Chromatographic workup (see above) gave 800 mg (0.91 mmol, 91%) **11e** in the form of orange-coloured oil. Anal. Found: C, 53.60; H, 5.28; N, 3.64%. $C_{40}H_{44}N_2OP_3F_6Rh$ (878.63): Anal. Calc.: C, 54.68; H, 5.05; N, 3.19%. MS (FAB), *m*/*z* (%) [frag.]: 733 (100) [{(**4a**)Rh(COD)}$^+$], 625 (96) [{(**4a**)Rh}$^+$], 547 (24) [{(**4a**)Rh}$^+$–Ph], 440 (25) [{(**4a**)Rh}$^+$–PPh_2]. ^{1}H-NMR (CD_2Cl_2): 2.01–2.50 (m, 14H, methylene–*H*(COD), CH_2P, CH_2N), 3.64 (m, 2H, CH_2O), 4.59 [m, 4H, olefin–*H*(COD)], 6.22 (s, 1H, C*H*pz), 7.29–7.81 (m, 22H, C*H*pz, aromatic *H*). ^{13}C-NMR (CD_2Cl_2): 27.4 (m, *C*H_2P), 30,5 [bs, $C_{methylene}$(*COD*)], 43.8 (s, *C*q), 58.3 (m, *C*H_2N), 65.9 (m, *C*H_2O), 102.1, 103.6 [2bs, C_{olefin}(*COD*)], 105.7, 105.9 (2s, *C*H(4)pz), 129.1–140.1 (m, aromatic *C*, *C*H(5)pz, *C*H(3)pz). ^{31}P-NMR (CD_2Cl_2): + 15.0 (d, 2P, $^1J_{RhP} = 143$ Hz), − 144.2 (sept, 1P, $^1J_{PF} = 712$ Hz, PF_6^-).

4.8. η^2-[1,1,1-Tris-(pyrazol-1-yl-methyl)ethan-rhodium(I)-η^4-1,5-cyclooctadiene] hexafluorophosphate (7f)

Compound **7f** was prepared as described above for **7a**. Starting materials: 270 mg (1 mmol) **3** ([7]b), 247 mg (0.5 mmol) di-μ-chloro-bis-(η^4-1,5-cyclooctadiene)-dirhodium(I), 190 mg (1.03 mmol) potassium hexafluorophosphate. Chromatographic workup (see above) gave upon removal of the solvent 610 mg (0.97 mmol, 97%) **7f** as a yellow microcrystalline solid. Recrystallisation afforded 490 mg (0.78 mmol, 78%) of **7f** in the form of yellow crystals suitable for X-ray structural analysis, m.p. 200–205°C (decomposition). Anal.

[2] Carbon and hydrogen values were notoriously low, presumably due to the incorporation of KCl.

Found: C, 41.91; H, 4.82; N, 13.20; P, 4.86%. $C_{22}H_{30}N_6PF_6Rh$ (626.39): Anal. Calc.: C, 42.18; H, 4.83; N, 13.42; P, 4.94%. MS (FAB), *m/z* (%) [frag.]: 481 (100) [{(**3**)Rh(COD)}$^+$], 373 (6) [{(**3**)Rh}$^+$]. ^{1}H-NMR ($CDCl_3$): 1.00 (s, 3H, CqCH_3), 2.06–2.71 (m, 8H methylene–*H*(COD), 4.27 [bs, 4H, olefin–*H*(COD)], 4.62 (m, 4H, CH_2N), 4.75, 5.63 (2bs, 2H, CH_2N), 6.41 (m, 3H, C*H(4)*pz), 7.54–8.38 (m, 6H, C*H(3)*pz, C*H(5)*pz). ^{13}C–NMR ($CDCl_3$): 18.5 (bs, CqCH_3), 31.0 [bs, $C_{methylene}$(*COD*)], 41.8 (s, *C*q), 60.9, 61.4 (2bs, *C*H_2N), 84.6, 86.9 [2bs, C_{olefin}(*COD*)], 106.3, 108.7 (2s, *C*H(4)pz), 132.9–140.7 (m, aromatic *C*, *C*H(5)pz, *C*H(3)pz). ^{31}P-NMR ($CDCl_3$): −143.9 (sept, $^1J_{PF}$ = 712 Hz, PF_6^-).

4.9. η^2-(P,N)-[2-(Diphenylphosphanylmethyl)-2,2-bis-(pyrazol-1-yl-methyl)-1-propanol-rhodium(I)-η^4-1,5-cyclooctadiene]hexafluorophosphate (**7g**)

Compound **7g** was prepared as described above for **7a**. Starting materials: 405 mg (1 mmol) **4b** ([7]b), 247 mg (0.5 mmol) di-μ-chloro-bis-(η^4-1,5-cyclooctadiene)-dirhodium(I), 190 mg (1.03 mmol) potassium hexafluorophosphate. Chromatographic workup (see above) gave upon removal of the solvent 620 mg (0.81 mmol, 81%) **7g** as a yellow microcrystalline solid. Recrystallisation at 0°C afforded 420 mg (0.55 mmol, 55%) of **7g** in the form of yellow crystals suitable for X-ray structural analysis, m.p. 170°C (decomposition). Anal. Found: C, 49.12; H, 5.15; N, 7.27; P, 7.97%. $C_{31}H_{37}N_4OP_2F_6Rh$ (760.50): Anal. Calc.: C, 48.96; H, 4.90; N, 7.37; P, 8.15%. MS (FAB), *m/z* (%) [frag.]: 615 (100) [{(**4b**)Rh(COD)}$^+$], 507 (21) [{(**4b**)Rh}$^+$]. ^{1}H-NMR (CD_2Cl_2): 2.21–2.90 (m, 10H, methylene–*H*(COD), CH_2N), 3.14, 5.05 [m, 4H, olefin–*H*(COD)], 3.72 (m, 2H, CH_2P), 4.43 (bs, O*H*), 5.19 (bs, 2H, CH_2O), 6.41 (s, 1H, $^3J_{HH}$ = 2.1 Hz, C*H*(4)pz), 7.49–7.97 (m, 14H, aromatic *H*, C*H*(3)pz, C*H*(5)pz). ^{13}C-NMR: no spectrum obtained because of the low solubility of **7f**. ^{31}P-NMR (CD_2Cl_2): +16.9 (d, 1P, $^1J_{RhP}$ = 147 Hz), −144.0 (sept, 1P, $^1J_{PF}$ = 712 Hz, PF_6^-).

4.10. η^2-P,N-[2-(Dimethylaminomethyl)-2-(diphenylphosphanylmethyl)-2-(3,5-dimethyl-pyrazol-1-yl-methyl)-ethan-rhodium(I)-η^4-1,5-cyclooctadiene]-hexafluorophosphate (**7h**)

Compound **7h** was prepared as described above for **7a**. Starting materials: 394 mg (1 mmol) **5** ([7]b), 247 mg (0.5 mmol) di-μ-chloro-bis-(η^4-1,5-cyclooctadiene)-dirhodium(I), 190 mg (1.03 mmol) potassium hexafluorophosphate. Chromatographic workup (see above) allowed the elution of **7d** as a sharp yellow band with dichloromethane/THF 1:1 which gave upon removal of the solvent 680 mg (0.90 mmol, 90%) **7h** as a yellow microcrystalline solid. m.p. 190°C (decomposition). Anal. Found: C, 49.32; H, 5.65; N, 4.10%. $C_{32}H_{44}N_3P_3F_6Rh$ (749.56): Anal. Calc.: C, 51.28; H, 5.92; N, 5.61%. MS (FAB), *m/z* (%) [frag.]: 604 (100) [{(**5**)Rh(COD)}$^+$], 494 (17) [{(**5**)Rh}$^+$]. ^{1}H-NMR ($CDCl_3$): 0.10 (s, 3H, CqCH_3), 1.73–3.09 [m, 24H, methylen–*H*(COD), CH_2P, CH_2N, NMe_2], 3.71, 4.86 [2m, 4H, Olefin–*H*(COD)], 4.55, 5.51 (2m, 2H, CH_2pz), 5.90 (bs, 1H, C*H*(4)pz), 7.20–7.89 (m, 10H, aromatic *H*). ^{13}C-NMR: no spectrum obtained because of the low solubility of **7h**. ^{31}P-NMR ($CDCl_3$): +16.2 (d, 1P, $^1J_{RhP}$ = 149.0 Hz), −144.2 (sept, 1P, $^1J_{PF}$ = 712 Hz, PF_6^-).

4.11. η^2-(P,O)-[2,2-Bis-(diethylaminomethyl)-3-(diphenylphosphanylmethyl)-1-propanol] rhodium (I)η^4-1,5-cyclooctadiene]hexafluorophosphate (**7i**)

Compound **7i** was prepared as described above for **7a**. Starting materials: 415 mg (1 mmol) **6** ([7]b), 247 mg (0.5 mmol) di-μ-chloro-bis-(η^4-1,5-cyclooctadiene)-dirhodium(I), 190 mg (1.03 mmol) potassium hexafluorophosphate. Chromatographic workup (see above) allowed the elution of **7i** as a sharp yellow band with dichloromethane/THF 1:1 which gave upon removal of the solvent 650 mg (0.84 mmol, 84%) **7i** as a yellow microcrystalline solid. Recrystallisation afforded 540 mg (0.70 mmol, 70%) of **7i** in the form of yellow needles suitable for X-ray structural analysis, m.p. 120–130°C (decomposition). Anal. Found: C, 51.09; H, 6.69; N, 3.59; P, 7.96%. $C_{33}H_{51}N_2P_2F_6Rh$ (770.62): Anal. Calc.: C, 51.43; H, 6.67; N, 3.64; P, 8.04%. MS (FAB), *m/z* (%) [frag.]: 625 (100) [{(**6**)Rh(COD)}$^+$], 513 (15) [{(**6**)Rh}$^+$], 415 (22) [(**6**)$^+$]. ^{1}H-NMR ($CDCl_3$): 1.11 (m, 12H, CH_2CH_3), 2.12–3.01 [m, 22H, methylene–*H*(COD), CH_2P, CH_2N, CH_2CH$_3$], 3.81 (s, 2H, CH_2O), 5.15 [m, 4H, olefin–*H*(COD)], 7.54–7.70 (m, 10H, aromatic *H*). ^{13}C-NMR ($CDCl_3$): 10.8 (s, NCH$_2$*C*H$_3$), 28.5 [bs, $C_{methylene}$(*COD*)], 31.0 (m, *C*H$_2$P), 33.1 (s, *C*H$_2$N), 42.0 (s, *C*q), 49.0 (s, N*C*H$_2$CH$_3$), 63.7 (s, *C*H$_2$O), 72.0 (bs, *C*H$_2$N), 108.2 [bs, C_{olefin}(*COD*)], 129.6–133.8 (m, aromatic *C*). ^{31}P-NMR ($CDCl_3$): +17.7 (d, 1P, $^1J_{RhP}$ = 164 Hz), −144.2 (sept, 1P, $^1J_{PF}$ = 710 Hz, PF_6^-).

4.12. Hydrogenation experiments

The hydrogenations were performed under the conditions given in Tables 2 and 3. Final conversions were determined by ^{1}H-NMR. The hydrogenations of diphenylacetylene were performed in a HR100 steel laboratory autoclave (Berghof/Maasen GmbH) equipped with a manometer and inlet and outlet valves. The solutions were prehydrogenated for 1 h at room temperature and normal pressure. The hydrogenations of (*Z*)-α-*N*-acetamidocinnamic acid were performed at

normal pressure in an hydrogenation apparatus after Marhan (Normag). The consumption of H_2 was monitored during the reaction.

Acknowledgements

We are grateful to the German Science Foundation (DFG), SFB 247, the VW Foundation (Stiftung Volkswagenwerk) and the Fonds der Chemischen Industrie for financial support. The technical support by Th. Jannack (mass spectrometry) and the Microanalytical Laboratory of the Institute of Organic Chemistry is gratefully acknowledged. We wish to thank Degussa AG for a generous loan of $RhCl_3 \cdot 3H_2O$.

References

[1] For representative reviews see: (a) L. Sacconi, F. Mani, Transition Met. Chem. 8 (1982) 179. (b) C. Bianchini, A. Meli, M. Peruzzini, F. Vizza, F. Zanobini, Coord. Chem. Rev. 120 (1992) 193. (c) H.A. Mayer, W.C. Kaska, Chem. Rev. 94 (1994) 1239.
[2] (a) S. Beyreuther, J. Hunger, G. Huttner, S. Mann, L. Zsolnai, Chem. Ber. 129 (1996) 745. (b) J. Hunger, S. Beyreuther, G. Huttner, J. Mol. Model. 2 (1996) 257. (c) S. Beyreuther, J. Hunger, G. Huttner, J. Mol. Model. 2 (1996) 273.
[3] (a) C. Bianchini, A. Meli, M. Peruzzini, Y. Fujiwara, T. Jintoku, H. Taniguchi, J. Chem. Soc. Chem. Commun. (1988) 299. (b) C. Bianchini, A. Meli, F. Laschi, J.A. Ramirez, P. Zanello, Inorg. Chem. 27 (1988) 4429. (c) C. Bianchini, A. Meli, M. Peruzzini, F. Vizza, P. Frediani, J. Ramirez, Organometallics 9 (1990) 226. (d) C. Bianchini, A. Meli, M. Peruzzini, F. Vizza, Organometallics 9 (1990) 2283. (e) J. Ott, G.M. Ramos Tombo, L.M. Venanzi, G. Wang, T.R. Ward, Tetrahedron Lett. 30 (1989) 6151. (f) V. Sernau, G. Huttner, M. Fritz, L. Zsolnai, O. Walter, J. Organomet. Chem. 453 (1993) C23.
[4] (a) G.G. Johnston, M.C. Baird, Organometallics 8 (1989) 1894. (b) C. Bianchini, K.G. Caulton, K. Folting, A. Meli, M. Peruzzini, A. Polo, F. Vizza, J. Am. Chem. Soc. 114 (1992) 7290. (c) J. Scherer, G. Huttner, O. Walter, B. Janssen, L. Zsolnai, Chem. Ber. 129 (1996) 1603. (d) J. Scherer, G. Huttner, M. Büchner, J. Bakos, J. Organomet. Chem. 520 (1996) 45.
[5] (a) E.G. Thaler, K. Folting, K.G. Caulton, J. Am. Chem. Soc. 112 (1990) 2664. (b) G. Kiss, I. Horváth, Organometallics 10 (1991) 3798.
[6] (a) A. Bader, E. Lindner, Coord. Chem. Rev. 108 (1991) 27. (b) W. Keim, Angew. Chem. 102 (1990) 251; Angew. Chem. Int. Ed. Engl. 29 (1990)235. (c) C. Abu-Gnim, I. Amer, J. Chem. Soc. Chem. Commun. (1994) 115.
[7] (a) A. Jacobi, G. Huttner, U. Winterhalter, Chem. Ber. 130 (1997) 1279. (b) A. Jacobi, G. Huttner, U. Winterhalter, S. Cunskis, Eur. J. Inorg. Chem. (1998) in press.
[8] G. Giordano, R.H. Crabtree, Inorg. Synth. 28 (1990) 88.
[9] J. Bakos, I. Tóth, B. Heil, G. Szalontai, L. Párkányi, V. Fülöp, J. Organomet. Chem. 370 (1989) 263.
[10] A.J. Canty, N.J. Minchin, J. Organomet. Chem. 226 (1982) C14.
[11] A.J. Canty, N.J. Minchin, J. Chem. Soc. Dalton Trans. (1986) 645.
[12] M.A. Esteruelas, L.A. Oro, J. Organomet. Chem. 366 (1989) 245.
[13] For a closer discussion and interpretation of the torsion angles in six-membered chelate cycles see Ref. ([7]a).
[14] M.J. Burk, J.E. Feaster, R.L. Harlow, Tetrahedron Asymmetry 2 (1991) 569.
[15] (a) M. Nogradi, Stereoselective Synthesis, 2nd ed., VCH, Weinheim, 1995. (b) J. Halpern, Asymmetric synthesis, in: J.D. Morrison (Ed.), Chiral Catalysis, vol. 5, Academic Press, New York, 1985, p. 41.
[16] J. Scherer, G. Huttner, H. Heidel, J. Organomet. Chem. 539 (1997) 67.
[17] F.H. Allen, J.E. Davies, J.J. Galloy, et al., J. Chem. Inf. Comput. Sci. 31 (1987) 187 (Cambridge Structural Database).
[18] Organikum, Deutscher Verlag der Wissenschaften, Berlin, 1990, p. 638.
[19] (a) G.M. Sheldrick, SHELXS-86, University of Göttingen, 1986. (b) G.M. Sheldrick, SHELX-93, University of Göttingen, 1993.
[20] L. Zsolnai, G. Huttner, XPMA, University of Heidelberg, 1994.